Spin coherence and formation dynamics of charged excitons in CdTe/Cd$_{1-x-y}$Mg$_x$Zn$_y$Te quantum wells

E. Vanelle, M. Paillard, X. Marie, and T. Amand

Laboratoire de Physique de la Matière Condensée, INSA-CNRS, Complexe Scientifique de Rangueil, 31077 Toulouse CEDEX, France

P. Gilliot, D. Brinkmann, and R. Lévy

IPCMS-GONLO, UMR 7504 CNRS et Université Louis Pasteur-Strasbourg, 23 rue du Loess, Boîte Postale 20 CR, 67037 Strasbourg CEDEX, France

J. Cibert and S. Tatarenko

Laboratoire de Spectrométrie Physique, CNRS et Université Joseph Fourier-Grenoble, Boîte Postale 87, 38402 Saint Martin d'Hères CEDEX, France

We report on a study of the spin coherence and on the formation dynamics of charged excitons in a p-doped CdTe/Cd$_{1-x-y}$Mg$_x$Zn$_y$Te quantum well by time-resolved photoluminescence under strictly resonant excitation of either the neutral or the charged exciton transition. The analysis of the decay of the charged exciton photoluminescence polarization and of the oscillation of this polarization when a transverse magnetic field is applied allows us to conclude that the formation of a charged exciton via an exciton state does not affect either the electron spin orientation or its coherence. The radiative lifetime of the charged exciton is directly measured and is found to be ~60 ps. Its formation time is determined from the experiments via a detailed model and is found to be ~65 ps. We also obtain information on the excitonic spin-flip time (12 ps) and the single-carrier spin-flip times within the exciton (electron, 60 ps and hole, 20 ps).

I. INTRODUCTION

Since their first experimental observation[1] charged excitons (X^+ or X^- for one electron bound to two holes or one hole bound to two electrons, respectively) have been recognized as essential for the understanding of the optical properties of a two-dimensional carrier gas, and have been the subject of numerous studies.[2–4] Recently, they have been used as a probe to characterize the electrostatic potential fluctuations in modulation-doped quantum wells (QW's).[5] The important role played by the charged excitons (also called trions) in the optical properties of quantum dots have also been revealed.[6] Only very few groups, however, have investigated their dynamical properties. Finkelstein *et al.*[7] have studied the formation process of X^- in modulated n-doped GaAs/Ga$_x$Al$_{1-x}$As QW's and found a X^- formation time of ~90 ps after resonant excitation of the X state. They also measured the X^- radiative lifetime and found ~60 ps at low temperature ($T=2$ K). Four-wave-mixing experiments have been performed on modulation p-doped CdTe/Cd$_{1-x-y}$Mg$_x$Zn$_y$Te QW's in order to measure the dephasing rate of the X^+.[8] They show that the X^+-X^+ collision processes are much less efficient than the X-X processes (the scattering cross section is one order of magnitude lower). This leads one to conclude to the localization of the X^+ in the electrostatic potential fluctuations induced by the ionized acceptors (see also Ref. 9 for the study of negatively charged excitons in ZnSe QW). Kossacki *et al.*[10] have studied the radiative lifetime of X^+ in CdTe/Cd$_{1-x-y}$Mg$_x$Zn$_y$Te QW's versus the two-dimensional (2D) hole concentration and found a constant value of 65 ps. To the best of our

knowledge, processes governing the spin dynamics and the spin coherence remain nevertheless largely unknown.

In this paper we report on time-resolved photoluminescence (PL) experiments in modulation p-doped CdTe/Cd$_{1-x-y}$Mg$_x$Zn$_y$Te QW's under resonant excitation of either X or X^+. In addition to the time behavior of either X or X^+ total intensity, we study and analyze the time dependence of their PL circular polarization and of the spin coherence when a transverse magnetic field is applied (Voigt configuration). In this case, well-defined oscillations are observed both on X and X^+ luminescence. In the case of X, they are attributed to exciton spin quantum beats.[11] In the case of X^+, they originate from the Larmor precession of the electron spin, hence we can extract a precise value of the electron g factor ($g_e=1.25\pm0.05$). Their amplitude is maximum[11,12] and we show that it comes from the vanishing of the exchange interaction between the electron and the two holes of opposite spin inside X^+. [Using a model developed earlier for excitons by Vinattieri *et al.*,[13] to analyze the PL dynamics on one hand and, on the other hand, extending the analysis of Dyakonov *et al.* for the spin coherence data, we obtain a fairly detailed description of the dynamics in the X-X^+ system in such quantum wells. We show that the creation of X^+ occurs with a typical time of ~65 ps, and does not affect either the spin orientation nor the spin coherence of the electrons. We also obtain information on the excitonic spin-flip time (12 ps), and the single-carrier spin-flip times (electron, 60 and hole, 20 ps). And finally we confirm the radiative lifetimes of the localized charged exciton (60 ps) and of the neutral exciton.

The paper is organized as follows: in Sec. II the sample
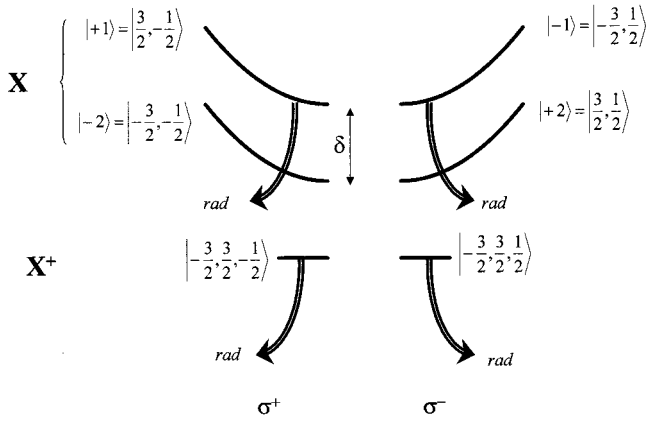
FIG. 1. Overall description of the X-X^+ level system (see text).

structure and the experimental setup are described. The experimental results are presented in Sec. III and analyzed in Sec. IV.

II. SAMPLE DESCRIPTION AND EXPERIMENTAL SETUP

The investigated sample was grown by molecular-beam epitaxy on a (001) $Cd_{0.88}Zn_{0.12}Te$ substrate. The detail of the structure was described in Ref. 14. It comprises five $Cd_{0.69}Mg_{0.23}Zn_{0.08}Te$/CdTe quantum wells. The barrier material is lattice matched to the substrate, thus the CdTe QW is under biaxial compression. In the following we note the growth axis z, x the direction of the applied magnetic field in the plane of the QW, and the third axis y. The QW thickness is 77 Å and the barriers are doped with nitrogen[15] on both sides of each QW, leaving 1000-Å-thick spacer layers. The acceptor density in the barriers has been measured on C-V profiles and has been found to be 3×10^{17} cm^{-3} and the estimated density of the two-dimensional hole gas in the QW's is $\sim 7 \times 10^{10}$ cm^{-2} (calculated at 0 K). This sample shows thus cw PL spectra with nearly equal X and X^+ intensities.

The X-X^+ system we will discuss is schematized in Fig. 1. The conduction band around its minimum is S-like, with two spin states $S_z = \pm \frac{1}{2}$. The valence band is split into a heavy-hole band with the total angular-momentum projection $J_{h-z} = \pm 3/2$ and a light-hole band with $J_{l-z} = \pm 1/2$. The coupling between the light- and the heavy-hole bands is expected to be very weak due to their large energy separation (~ 50 meV, as a consequence of both the quantum confinement and of the strain effects). Thus the neutral excitons X involved in this study are formed with heavy holes and can thus be described using the basis set $|J_z, S_z\rangle$ where $J_z \equiv J_{h-z}$. The exciton total angular-momentum projection ($J_z + S_z$) takes the values ± 1 and ± 2. The state $|+1\rangle = |+3/2, -1/2\rangle$ is radiative in the σ^+ polarization (and the state $|-1\rangle$ in σ^- polarization), if its in-plane wave vectors ($K_\parallel$) matches that of light or if it is localized. Free excitons with larger wave vectors, as well as $|\pm 2\rangle$ excitons, are non-radiative. The splitting between the $|\pm 1\rangle$ doublet and the $|\pm 2\rangle$ states is the zero-field exchange splitting δ (the small splitting between the two dark singlets will be neglected in the following).[16] We have also to consider the two "singlet" states (i.e., with respect to the hole states) which form the

ground level of X^+. They can be written as $1/\sqrt{2}\{|3/2, -3/2, 1/2\rangle - |-3/2, 3/2, 1/2\rangle\}$ and $1/\sqrt{2}\{|3/2, -3/2, -1/2\rangle - |-3/2, 3/2, -1/2\rangle\}$. The trion states were found, by four-wave mixing,[17] to be localized and both trion states are thus expected to be radiative.

For the time-resolved PL experiments, the sample was immersed in superfluid helium at 1.7 K and the magnetic field was applied perpendicular to the growth direction (Voigt configuration) using a superconducting magnet. The sample was excited by 1.4 ps pulses generated by a tunable titanium-sapphire laser at a repetition rate of 80 MHz. The spectral width of the excitation pulse was about 2 meV. The titanium-sapphire beam is also used to synchronously pump an optical parametric oscillator (OPO). The OPO pulse is used to up-convert the PL signal in a LiIO$_3$ nonlinear crystal. The overall time resolution, measured with a cross-correlation experiment, is 1.5 ps. This two-color up-conversion technique is necessary to record the X or X^+ PL transient when the excitation energies are resonant with the X or X^+ transitions.[18] Indeed, the spectral selectivity of the overall setup allows us to excite the X or the X^+ states and detect their PL separately, and thus to study the X PL dynamics after a resonant excitation of X [noted $X(X)$ in the following], the X^+ PL dynamics after a resonant excitation of X [noted $X^+(X)$], and the X^+ PL dynamics after a resonant excitation of X^+ [noted $X^+(X^+)$]. In all the experiments the laser was circularly polarized (σ^+) and the PL components of opposite helicities, I^+ and I^- corresponding to σ^+ and σ^-, respectively, were separated using a $\lambda/4$ plate and the frequency-mixing selection rules in the LiIO$_3$ crystal which acts as an analyzer. The circular polarization of the PL signal is defined as $P = (I^+ - I^-)/(I^+ + I^-)$. For the cw PL experiments the sample was mounted on a cold finger (the temperature was 10 K) and excited by a continuous tunable Ti-sapphire laser. The PL was dispersed through a double monochromator and detected using a cooled germanium photodiode.

III. EXPERIMENTS

Figure 2(a) shows the cw PL spectrum recorded at 10 K under low excitation density. The full width at half maximum (FWHM) of the X^+ and X lines is 1.7 meV and they are separated by 2.7 meV (the X^+ binding energy). PL excitation spectra (not shown) demonstrate that there is no measurable Stokes shift of X and X^+. Figure 2(b) shows time-resolved PL spectra recorded 75 ps after the excitation pulse in resonance with X (open circles) or X^+ (open triangles) at 1.7 K. The excitation power was 0.1 and 0.65 mW, respectively, resulting in initial densities of photogenerated $X(X)$ or $X^+(X^+)$ being both approximately 10^9 cm^{-2}. These densities are almost equal due to the difference in absorption coefficients. They are at least one order of magnitude smaller than the density of the two-dimensional hole gas, thus we can rule out any saturation of the X^+ transition. The linewidths are larger in the time-resolved spectra than in the cw one, due to the 3-meV spectral resolution of the experimental setup. Nevertheless the X and X^+ components are clearly separated, which makes it possible to study the PL dynamics of the X and X^+ lines independently. Arrow 1 indicates the central excitation and detection photon energies used to
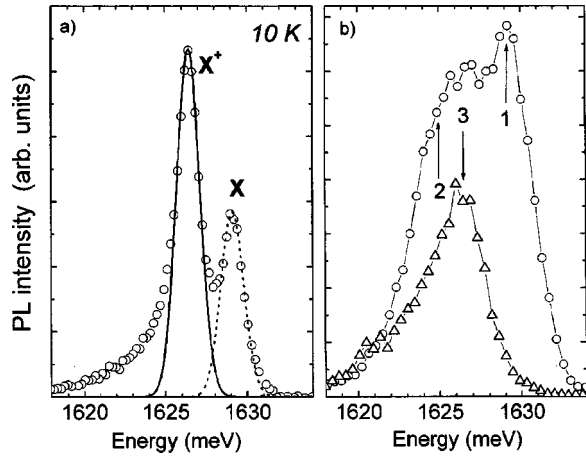
FIG. 2. (a) Circles: cw photoluminescence spectrum; full line and dashed line: Gaussian fit of the X^+ and X lines. (b) Time-resolved PL spectra at a delay 75 ps. Triangles: excitation in the charged exciton line at 1626.4 meV; circles: excitation in the neutral exciton line at 1629.2 meV. Arrows indicate the excitation-detection energies used in the time-resolved experiments (see text).

study the dynamics of X under resonant X excitation $[X(X)]$, arrow 2 the detection energy used to study X^+ under resonant X excitation $[X^+(X)]$, and arrow 3 the detection energy used to study X^+ under resonant X^+ excitation $[X^+(X^+)]$.

The FWHM of the $X^+(X^+)$ PL spectrum is 3.5 meV (resulting from the convolution of the instrumental response with the X^+ line shape) and there is no exciton contribution to the PL. We have checked that this is true regardless of the time delay. We have also checked carefully that the dynamics of the X^+ PL does not depend on the detection photon energy.

Figure 3(a) summarizes the dynamics of the total PL intensity ($I^+ + I^-$ components) of $X(X)$, $X^+(X)$ and $X^+(X^+)$. When exciting in resonance with the neutral exciton, the $X(X)$ PL intensity exhibits a fast initial drop before the decay becomes monoexponential, with a time constant of ~ 130 ps. This is due to the thermalization of the cold, optically active, excitons photogenerated by the resonant laser excitation, towards dark exciton states (i.e., $|\pm 1\rangle$ excitons with $K_\parallel > K_0$, where K_0 is the wave vector corresponding to the homogenous linewidth Γ_H, and $|\pm 2\rangle$ excitons). This transfer
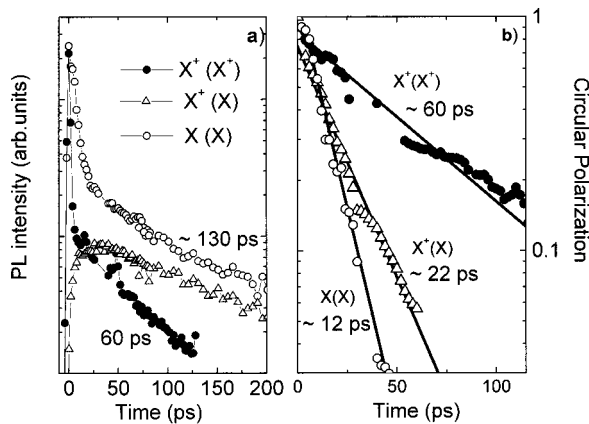
FIG. 3. PL dynamics: (a) total intensities, (b) polarization ratio.

to the exciton dark states as well as the radiative recombination of the optically active excitons leads to the fast and strong initial drop of the $X(X)$ PL intensity, as first observed by Deveaud *et al.*[19] Our time resolution allows us to resolve the rise time of the $X^+(X)$ PL ($\tau_{\rm rise} \sim 13$ ps). We shall show below that this rise time is not determined by the formation time of the trion, but is defined by the spreading of excitons over the k space. At long time the $X^+(X)$ PL decays with the same time constant, ~ 130 ps, as that of the $X(X)$ PL. This decay time represents an average over all exciton states and it is significantly longer than the $X^+(X^+)$ one, as previously observed in Ref. 7. When exciting directly the trion $[X^+(X^+)$ signal], its PL intensity decays monoexponentially with a time constant of 60 ps (the spike observed at $t=0$ is due to the laser light backscattered from the sample surface). We can thus conclude that all the photogenerated X^+ remain optically active or that an equilibrium between optically active and nonactive X^+ is reached during the first couple of picoseconds after the excitation pulse. For the present sample this decay time can be regarded as a direct measure of the radiative lifetime of the X^+ as we shall see that there is no optically non-active X^+ states. Indeed, the stable state of the X^+ is formed with an electron and two holes of opposite spins (singlet state). Thus whatever the electron spin state is, the X^+ is always optically active. For free charged excitons the oscillator strength is expected to decrease for large wave vector[20] and a thermalization in the k space should also lead to a nonexponential decay of the $X^+(X^+)$ PL in the present experiment. However, as the X^+ studied in our sample are localized,[17] they are optically active and there is thus no dark states at all for the charged excitons. The same decay time was observed by Kossacki *et al.*[10] in quite similar samples, independently of the hole density.

Figure 3(b) illustrates the decay of the circular polarization. The excitonic polarization $[X(X)$ spectrum] decreases with a time constant of 12 ps, four times shorter than in typical III-V QW's of comparable sizes.[13] As the X are created resonantly, i.e., without kinetic energy, this time reflects mainly the excitonic spin-flip time τ_X (i.e., the simultaneous spin flip of the electron and the hole within an exciton).[12,13,21] The $X^+(X^+)$ circular polarization decreases with a significantly longer time (60 ps). As the X^+ is formed with two heavy holes of opposite spin (i.e., $J_z = +\frac{3}{2}$ and $J_z = -\frac{3}{2}$, respectively), this polarization behavior reflects the spin relaxation τ_e of the electron only. The polarization decay time of the X^+ generated via X states $[X^+(X)$ spectrum] is intermediate, with an average time constant ~ 22 ps. This intermediate behavior originates directly from the continuous creation of X^+ by the neutral X: X^+ created at short times $t < \tau_X$ result from highly polarized X and those retain their polarization for quite a long time (τ_e), while nonpolarized X^+ are generated at slightly longer delays from excitons that have already lost their spin orientation. The fact that the $X^+(X)$ exhibits a strong initial polarization shows that the creation of X^+ via X states does not affect the spin orientation.

Figure 4 shows the time dependence of the PL circular polarization when a 4 T transverse magnetic field is applied (closed circles). The circular polarization with no magnetic field (open circles) is also plotted for comparison. Figure 4(a) illustrates the $X(X)$ configuration. The observed oscilla-
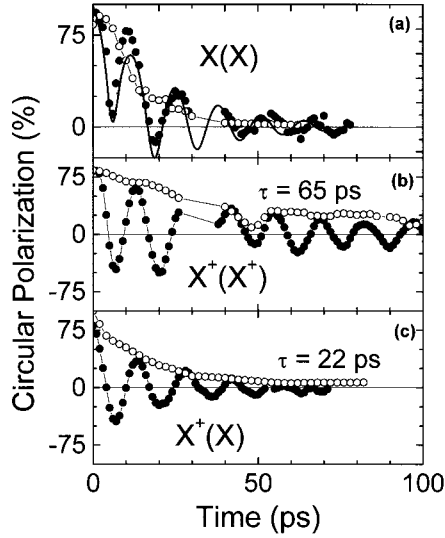
FIG. 4. PL polarization dynamics with (closed symbols) and without (open symbols) applied magnetic field: (a) excitation and detection on the neutral exciton resonance, (b) excitation and detection on the charged exciton resonance, (c) excitation on the neutral exciton resonance and detection on the charged exciton resonance. The solid line in (a) is a fit described in Sec. III B. The data around 30 ps have been removed because of a reflection of the excitation laser beam on the back of the sample.

tions are not symmetric and this shows that they originate from the exciton spin quantum beats as initially observed in GaAs/Ga$_x$Al$_{1-x}$As QW's.[11,12] Surprisingly, the PL intensity at the polarization maxima is higher than in the $B=0$ T case at the same delay. This effect will be interpreted in the next section.

Figure 4(b) shows the behavior of the $X^+(X^+)$ PL polarization. In this case the period of the oscillations is a linear function of the inverse of the applied field (Fig. 5). The amplitude is maximum and we will show later that these oscillations originate from the Larmor precession of the electron spin only, as a consequence of the vanishing of the exchange interaction between the electron and the two holes of opposite spin inside X^+. The damping of the oscillations is here equal to the decrease of the circular polarization of the $X^+(X^+)$ PL without applied magnetic field. Finally Fig. 4(c) illustrates the $X^+(X)$ configuration. The oscillations are
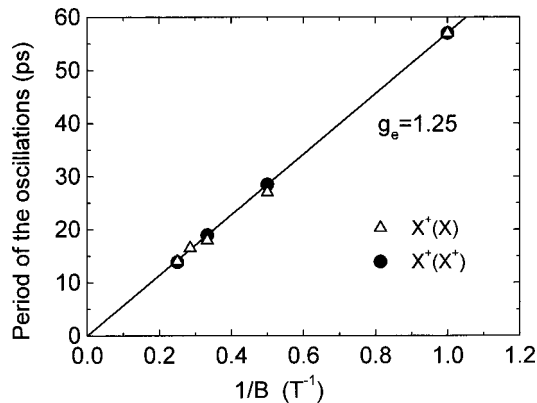
FIG. 5. Period of the X^+ polarization oscillation as a function of the inverse of the applied magnetic field.

of the same kind as in the $X^+(X^+)$ case, but the damping is faster. Here it is also equal to the decrease of the circular polarization of the $X^+(X)$ PL without applied magnetic field. We will show in the next section that this point allows us to conclude that the creation of X^+ from X does not affect the spin coherence of electrons.

IV. DETAILED ANALYSIS

A. Period of the polarization oscillations of X^+

In order to explain the oscillations observed in Fig. 4(b) [$X^+(X^+)$ configuration], we have to describe how the X^+ interacts with the applied field. We start with the effective spin Hamiltonian of X,[13] which includes the electron-hole exchange interaction and the Zeeman splitting under a transverse magnetic field (parallel to x),

$$H_{X-B} = -\frac{2\delta}{3} J_z S_z + \hbar \omega S_x, \quad (1)$$

where δ is the zero-field exchange splitting between the optically active doublet $|\pm 1\rangle = |\pm\frac{3}{2}, \mp\frac{1}{2}\rangle$ and the two closely lying singlet states $|\pm 2\rangle = |\pm\frac{3}{2}, \pm\frac{1}{2}\rangle$. We have defined $\hbar\omega = g_e \mu_B B$, where g_e is the electron Lande factor, B the applied magnetic field, and μ_B the Bohr magneton. We neglect the Zeeman effect on the hole, as the transverse hole g factor is vanishingly small in 2D structures.[22–24] For X^+ states, $|h_1, h_2, e\rangle$, the spin Hamiltonian becomes

$$H_{X^+-B} = -\frac{2\delta}{3}(J_z^1 S_z + J_z^2 S_z) + \hbar\omega S_x. \quad (2)$$

Evaluating this Hamiltonian between the X^+ ground states, $1/\sqrt{2}\{|\frac{3}{2}, -\frac{3}{2}, \frac{1}{2}\rangle - |-\frac{3}{2}, \frac{3}{2}, \frac{1}{2}\rangle\}$ and $1/\sqrt{2}\{|\frac{3}{2}, -\frac{3}{2}, -\frac{1}{2}\rangle - |-\frac{3}{2}, \frac{3}{2}, -\frac{1}{2}\rangle\}$, shows that the electron-hole exchange interaction vanishes, so that the restriction to the X^+ ground doublet simply writes

$$H_{X^+-B} = \hbar\omega S_x, \quad (3)$$

which is identical to the spin Hamiltonian of a single electron. Thus, the Larmor precession of the electron spin yields oscillations of the X^+ polarization with the electronic pulsation ω.[25] Figure 5 displays the oscillation period as a function of $1/B$. The slope is constant and gives a direct measure of the inverse of the Lande factor of the electrons. We measure $g_e = 1.25 \pm 0.05$. In Ref. 26 the author measured $g_e = 1.4$ in an undoped 80-Å width CdTe/Cd$_{0.75}$Mg$_{0.25}$Te QW, and in Ref. 27 they measured $g_e = 1.461$ in an n-doped 80-Å width CdTe/Cd$_{0.7}$Mg$_{0.3}$Te QW. This discrepancy is probably not due to variation of the confinement energy,[28] but may be induced by the doping.[29]

B. Exciton spin quantum beats

The oscillations observed in Fig. 4(a) [$X(X)$ configuration] originate from the spin quantum beats of the excitons as previously demonstrated in GaAs/Ga$_x$Al$_{1-x}$As QW's.[11,12] The transverse magnetic field mixes the $|+1\rangle$ and $|+2\rangle$ states, thus the photogeneration of nonstationary $|+1\rangle$ exciton states results in oscillations between the $|+1\rangle$ and $|+2\rangle$ components
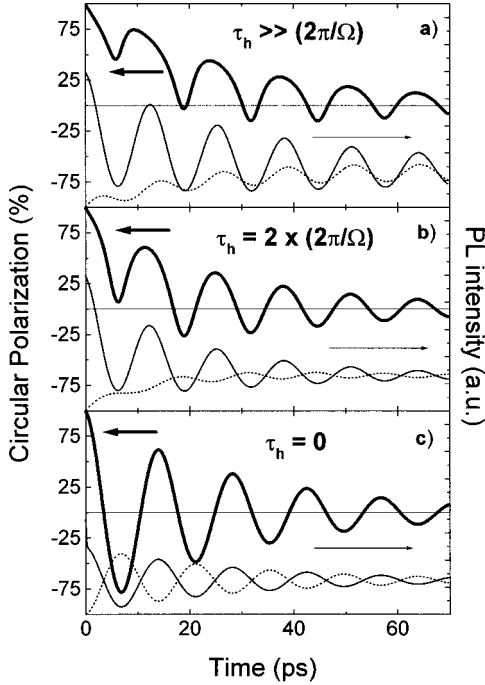
FIG. 6. Calculated polarization of the *X* PL in three special cases, assuming slow (a), intermediate (b), or infinitely fast (c) hole spin relaxation. Thick solid lines: circular polarization; thin solid lines: σ^+ PL intensity; thin dashed lines: σ^- PL intensity.

of the exciton wave function. For infinite values of the single-particle electron spin-flip time τ_e, hole spin-flip time τ_h, and exciton spin-flip time τ_x, an initial population of excitons in the $|+1\rangle$ state results in a PL intensity signal given for the two helicities by

$$I^+(t) = 1 - \left(\frac{\omega}{\Omega}\right)^2 \left(\frac{1 - \cos(\Omega t)}{2}\right),$$

$$I^-(t) = 0, \qquad (4)$$

where $\hbar\Omega = \sqrt{(\hbar\omega)^2 + \delta^2}$. Note that the amplitude of the oscillation is reduced by a factor $(\omega/\Omega)^2$, as a result of the small mixing induced by the transverse field. We estimate the value of the exchange energy δ for the present system to be 0.14 meV (see the Appendix).

In order to have a quantitative description of the excitonic spin quantum beat dynamic, we have improved the theory developed by Dyakonov *et al.*[12] by taking into account the excitonic spin flip and the single-particle electron spin flip. We can restrict ourselves to the subset formed by the $|\pm1\rangle$ and $|\pm2\rangle$ exciton states. We also include the radiative decay of the $|\pm1\rangle$ exciton and the formation of X^+. The $K_\parallel > K_0$ nonradiative states of the exciton are not taken into account here but we have checked that they have a very weak influence on the calculation.

Before detailing the model we give the results for three important simple cases (Fig. 6). In these three examples, we kept τ_e as well as the *X* radiative lifetime, $\tau_{\text{rad-}X}$, infinite, but all the other parameters have values adapted to the present system, i.e., $g_e = 1.25$, $B = 4$ T, $\tau_x = 12$ ps, and $\delta = 0.14$ meV. The first case, displayed in Fig. 6(a), corresponds to $\tau_h \gg 1/\Omega$, i.e., strongly correlated electron and hole

spins. Due to the finite spin-flip time of the exciton (τ_x), the σ^- component also oscillates. However, the excitonic nature of the quantum beats results in strongly nonsymmetric oscillations of the circular polarization. For intermediate values of τ_h with respect to $1/\Omega$, the situation becomes more complex. For the electron, the exchange interaction with the hole is equivalent to a magnetic field applied along the growth direction $B_{ex} = \delta/(g_e\mu_B)$. The hole spin flip makes this magnetic field to flip also. Thus, if τ_h becomes very short compared to $1/\Omega$, i.e., compared to the precession time of the electron within the exciton, the average effect of B_{ex} vanishes, and we recover the Larmor precession of the electron. Figures 6(b) and 6(c) display the intermediate case $\tau_h/(2\pi/\Omega) = 2$ (which corresponds to $\tau_h = 26$ ps in our case) and the limiting case $\tau_h = 0$, respectively. Note also that compared to usual III-V systems, the electron *g* factor is strong [1.25 compared to ~0.25 (Refs. 11 and 30)], hence the effect of δ on the oscillation period is small (the period of the electron spin quantum beats is 14 ps compared to 13 ps for the excitonic ones). The result shown in Fig. 4(a) clearly belongs to the intermediate case.

We now turn to the quantitative fit using the theory adapted from Ref. 12, including the excitonic spin relaxation time and the single-particle spin relaxation time of the electron. We use the density-matrix formalism and the notations of Ref. 12. Overlined indexes in density-matrix elements indicates negative excitonic spin states.

The excitonic spin flip (between the $|+1\rangle$ and $|-1\rangle$ states) is known to be mainly due to the electron-hole long-range interaction within the exciton.[21] Its effect can be described as follows:

$$\left.\frac{\partial\rho_{11}}{\partial t}\right)_X = -\frac{\rho_{11} - \rho_{\bar{1}\bar{1}}}{2\tau_X},$$

$$\left.\frac{\partial\rho_{\bar{1}\bar{1}}}{\partial t}\right)_X = -\frac{\rho_{\bar{1}\bar{1}} - \rho_{11}}{2\tau_X}, \qquad (5)$$

which describe the evolution of the populations of the $|+1\rangle$ and $|-1\rangle$ states and,

$$\left.\frac{\partial\rho_{22}}{\partial t}\right)_X = \left.\frac{\partial\rho_{\bar{2}\bar{2}}}{\partial t}\right)_X = 0, \qquad (6)$$

which describes the fact that the long-range interaction between the electron and the hole does not operate between the $|\pm2\rangle$ states,[21] so that the spin-flip mechanism is inhibited for these states and

$$\left.\frac{\partial\rho_{12}}{\partial t}\right)_X = -\frac{\rho_{12}}{4\tau_X}. \qquad (7)$$

Identical equations hold for ρ_{21}, $\rho_{\bar{1}\bar{2}}$, and $\rho_{\bar{2}\bar{1}}$. We assume that, in our conditions, $\rho_{\bar{1}2} \ll \rho_{12}$. As a matter of fact, one could imagine that an excitonic spin flip would lead to the creation of a $\rho_{\bar{1}2}$ coherence with a preexisting ρ_{12}. In our experimental conditions, the exciton quantum beats between $|+1\rangle$ and $|+2\rangle$ states occur at a period $2\pi/\Omega$ shorter than $4\tau_x$ (15 and 48 ps, respectively) so that the coherence term $\rho_{\bar{1}2}$ cannot ''follow'' the oscillations. As the spin flip occurs at

an arbitrary time, the initial phase between the $|+1\rangle$ and $|+2\rangle$ states is also arbitrary and thus no coherence is generated.[31]

The single-particle spin-flip time of the electron is introduced in the following way:

$$\left.\frac{\partial \rho_{11}}{\partial t}\right)_e = -\left.\frac{\partial \rho_{22}}{\partial t}\right)_e = -\frac{\rho_{11} - \rho_{22}}{2\tau_e},$$

$$\left.\frac{\partial \rho_{\bar{1}\bar{1}}}{\partial t}\right)_e = -\left.\frac{\partial \rho_{\bar{2}\bar{2}}}{\partial t}\right)_e = -\frac{\rho_{\bar{1}\bar{1}} - \rho_{\bar{2}\bar{2}}}{2\tau_e}, \quad (8)$$

and

$$\left.\frac{\partial \rho_{12}}{\partial t}\right)_e = -\frac{\rho_{12}}{\tau_{e\perp}} = -\frac{\rho_{12}}{2\tau_e}, \quad (9)$$

and identical equations for ρ_{21}, $\rho_{\bar{2}\bar{1}}$, and $\rho_{\bar{2}\bar{1}}$. The factor $\tau_{e\perp}$ is the transverse electron spin-flip time which governs the relaxation of $\langle S_x \rangle$ and $\langle S_y \rangle$, hence that of ρ_{ij} [$(i;j) = (1;2),(2;1),(\bar{1};\bar{2}),(\bar{2};\bar{1})$]. Dyakonov and Kachorovski[32] have shown that $\tau_{e\perp} = 2\tau_e$, where τ_e is the longitudinal electron spin-flip time, i.e., the one which governs the relaxation of S_z, and hence describes the decay of the X^+ circular polarization, which was determined in Sec. II from time-resolved PL experiments without applied field.

Here $\langle \vec{S} \rangle$ is the total value of the spins of the electrons within the excitons. $\langle \vec{S} \rangle$ and the exciton density N_X can be expressed using the density-matrix components

$$\langle S_x \rangle = \tfrac{1}{2}(\rho_{12} + \rho_{\bar{1}\bar{2}} + \rho_{21} + \rho_{\bar{2}\bar{1}}),$$

$$\langle S_y \rangle = \tfrac{1}{2}(-\rho_{12} + \rho_{\bar{1}\bar{2}} + \rho_{21} - \rho_{\bar{2}\bar{1}}),$$

$$\langle S_z \rangle = \tfrac{1}{2}(-\rho_{11} + \rho_{\bar{1}\bar{1}} + \rho_{22} - \rho_{\bar{2}\bar{2}}),$$

$$N_X = \rho_{11} + \rho_{\bar{1}\bar{1}} + \rho_{22} + \rho_{\bar{2}\bar{2}}. \quad (10)$$

Finally we have to take into account the escape to the X^+ states. Because the hole Zeeman splitting is negligible, we do not expect any polarization of the hole gas, and thus the behavior of the X^+ is expected to be the same in both polarizations σ^+ and σ^-.[33] This means that we include the charged excitons in our model by simply adding the following term:

$$\left.\frac{\partial \rho_{ij}}{\partial t}\right)_{X^+} = -\frac{\rho_{ij}}{\tau_{\text{form}}}. \quad (11)$$

For $i = j$, this equation means that the populations of the $|\pm 1\rangle$ and $|\pm 2\rangle$ states decrease with the time constant τ_{form}, the formation time of X^+, assumed to be the same for all states. For $i \neq j$, this assumes that the decrease of the coherence induced by the formation of X^+ is also governed by the same τ_{form}. This equation is built in complete analogy with the evolution of ρ_{ij} due to the radiative recombination process, relying upon the fact that there are no forbidden states for the creation of X^+. Because all ρ_{ij} components are affected in the same way by the formation of X^+, this mechanism has no influence on the polarization behavior of X.

Without any calculation, we can now understand, qualitatively, why the $X(X)$ polarization can be higher in a transverse magnetic field than in $B = 0$ T [Fig. 4(a)]. This is a direct consequence of the excitonic nature of the quantum beats. As seen before, the long-range interaction between the electron and the hole, which is responsible for the X spin flip in the $|\pm 1\rangle$ subspace, does not operate in the $|\pm 2\rangle$ subspace. As a result, the depolarization mechanism, which fully operates at $B = 0$ T, is inhibited under the applied field each time the excitonic wave function is mainly $|+2\rangle$ due to the oscillations.

The solid line in Fig. 4(a) shows the best fit of the $X(X)$ polarization dynamics. The values of parameters are the following: $B = 4$ T, $g_e = 1.25$, $\tau_e = 60$ ps, $\tau_X = 12$ ps, $\delta = 0.14$ meV, $\tau_{\text{rad-}X} = 16$ ps, and $\tau_h = 20$ ps. The value of $\tau_{\text{rad-}X}$ is deduced from the fit of the PL dynamics described later, but we have checked that as soon as $\tau_{\text{rad-}X}$ is larger than half an oscillation period ($\sim$7 ps), its influence on the polarization dynamics is very weak. This is linked to the fact that after half a period the excitons, photogenerated as $|+1\rangle$, are mainly in the $|+2\rangle$ state and are no more radiative. Thus the only sensitive parameter in the calculation is τ_h (as shown in Fig. 6). The agreement between theory and experimental results is good. In particular, we are able to explain the enhancement of the polarization when a transverse magnetic field is applied. Nevertheless we would like to point out that this model remains a quite simplified way to describe the $X(X)$ polarization behavior. For instance it is now well established that, within the exciton, τ_h is extremely sensitive to the kinetic energy: as soon as the exciton is generated nonresonantly, τ_h becomes extremely short and the oscillation of the X PL under transverse magnetic field originates from the Larmor precession of the electron only.[11,34] In the present study, the excitons are generated with $K_\parallel < K_0$ but are spread over the $K_\parallel > K_0$ states shortly afterwards. We should then consider that τ_h depends on the kinetic energy. Taking into account this effect would lead us to introduce new adjustable parameters in the model, whereas it is expected to be small at 1.7 K. In the present model, τ_h should be considered as an effective hole spin-flip time, resulting of an average over the whole distribution of excitons. The oversimplification of our model, however, probably explains why we are unable to reproduce the very high polarization observed around $t = 10$ ps.

C. The spin coherence in X^+

The same model can be used to determine whether or not the electron coherence which exists within the photocreated exciton is destroyed when this exciton bounds to a hole to form a charged exciton. We have to add the master equations for the X^+ states, which we shall describe using the same macroscopic observables as defined above for the neutral exciton, i.e., $\langle \vec{S}^{X^+} \rangle$ (the total electron spin within the X^+), and N_{X^+} (the density of X^+). The set of coupled differential equations now reads

$$\frac{d\langle S_y^{X^+} \rangle}{dt} = -\omega \langle S_z^{X^+} \rangle - \frac{\langle S_y^{X^+} \rangle}{\tau_{\text{rad-}X^+}} + \beta \frac{\langle S_y \rangle}{\tau_{\text{form}}},$$

$$\frac{d\langle S_z^{X^+} \rangle}{dt} = +\omega \langle S_y^{X^+} \rangle - \frac{\langle S_z^{X^+} \rangle}{\tau_{\text{rad-}X^+}} + \frac{\langle S_z \rangle}{\tau_{\text{form}}}, \quad (12)$$

and
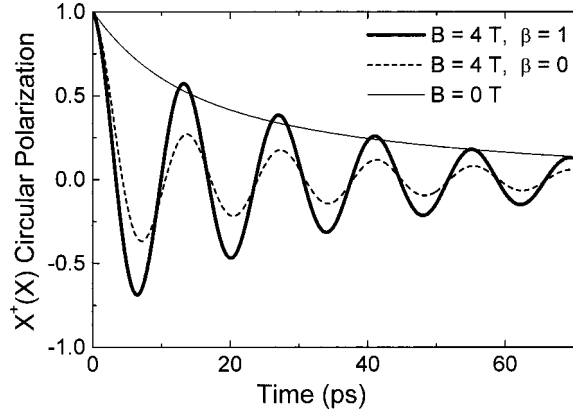
FIG. 7. Calculated polarization of the $X^+(X)$ PL, without and with the magnetic field assuming total loss ($\beta=0$) or total conservation ($\beta=1$) of the electron coherence during the creation of the charged exciton.

FIG. 8. Model of the dynamics in the X-X^+ system.

$$\frac{dN_{X^+}}{dt} = -\frac{N_{X^+}}{\tau_{\text{rad-}X^+}} + \frac{N_X}{\tau_{\text{form}}}, \qquad (13)$$

where $\tau_{\text{rad-}X^+}$ is the radiative life time of X^+ and $\beta=1$ if the formation of X^+ occurs without any loss of spin coherence, and $\beta=0$ if the electron spin coherence is completely lost. The parameter β does not appear in the differential equation which governs the evolution of $\langle S_z^{X^+} \rangle$ because the $X^+(X)$ PL polarization dynamics has shown that the formation of X^+ via a X state does not affect the spin orientation. Figure 7 displays the $X^+(X)$ polarization calculated in three cases: $B=0$ T (thin solid line), $B=4$ T, and $\beta=1$ (thick line), $B=4$ T, and $\beta=0$ (dashed line). The value of τ_{form} has only a weak influence on the calculated X^+ PL polarization as long as it remains long compared to $\sim \tau_{\text{rad-}X}$; in this case the formation of the trions do not modify significantly the evolution of the density of excitons. We use here $\tau_{\text{form}}=65$ ps, as obtained later in this section. Quite surprisingly, clear oscillations of the $X^+(X)$ polarization would be observed even if the coherence was fully lost. The main reason for this behavior is the very fast decay of N_X in the first ten picoseconds. The majority of the X^+ are thus generated immediately after the excitation, with an average electron-spin close to $+\frac{1}{2}$, whatever the efficiency of the coherence transfer is. The second reason comes from the very close values of the electron and exciton oscillation periods, 14 and 13 ps, respectively (which would not be true in GaAs/Ga$_x$Al$_{1-x}$As QW's, where the g factor is about ten times smaller than in the present system, and where we would have around 140 and 29 ps, respectively). The generation of X^+ via X states results in the formation of σ^+ emitting X^+ when the excitons are mainly in a $|+2\rangle$ or $|-1\rangle$ state, and in the formation of σ^- emitting X^+ when the excitons are mainly in a $|-2\rangle$ or $|+1\rangle$ state. Because the oscillation periods are almost identical, only few additional trions are generated with polarizations differing from the polarization which is defined by the oscillations initiated by the fast initial generation of polarized X^+. Nevertheless, as shown in Fig. 7, the oscillations are significantly weaker when the coherence is lost. The comparison with the experimental results displayed in Fig. 4(c) allows us to conclude that the formation of X^+ occurs with a
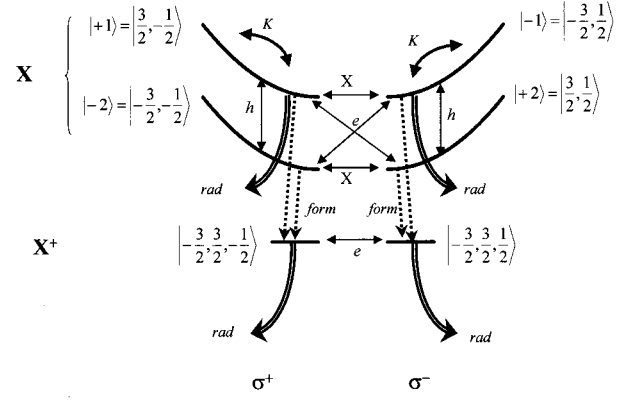
very good transfer of coherence. Indeed the maxima of the observed oscillations always correspond to the values measured without magnetic field, like in the case $\beta=1$ in Fig. 7.

D. PL dynamics

In order to extract the formation time of the X^+ and to understand the whole dynamics of the X-X^+ system, we have to consider the whole set of processes described in Fig. 8.[11] Only excitons with kinetic energy less than the homogeneous linewidth Γ_H (corresponding to $K_\parallel < K_0$) can radiatively recombine. We note τ_K the exciton thermalization time. The X^+ are formed only from excitons with $K_\parallel < K_0$; this process characterizes the parameter τ_{form} defined above [excitons with $K_\parallel > K_0$ have a negligible contribution to the formation of X^+ (Ref. 7)]. Double arrows in Fig. 8 mean that we have taken into account the reverse process, weighted by a thermal factor [for instance, $W_h^{\text{down}}=1/2\tau_h$ and $W_h^{\text{up}}=(1/2\tau_h)\exp(-\delta/k_B T)$]. The system is thus described by ten coupled differential equations. As an example the equation that drives the population of the $|+1\rangle$ excitons with $K_\parallel < K_0$ is

$$\frac{dN(+1,K_\parallel<K_0)}{dt} = -N(+1,K_\parallel<K_0)\left[\frac{1}{2\tau_h}+\frac{1}{2\tau_e}+\frac{1}{2\tau_X}\right.$$
$$\left.+\frac{1}{2\tau_k}+\frac{1}{\tau_{\text{form}}}+\frac{1}{\tau_{\text{rad-}X}}\right]$$
$$+\frac{N(-2,K_\parallel<K_0)}{2\tau_h}\left[\exp\left(\frac{-\delta}{k_B T}\right)\right]$$
$$+\frac{N(+2,K_\parallel<K_0)}{2\tau_e}\left[\exp\left(\frac{-\delta}{k_B T}\right)\right]$$
$$+\frac{N(-1,K_\parallel<K_0)}{2\tau_X}$$
$$+\frac{N(+1,K_\parallel>K_0)}{2\tau_k}\left[\exp\left(\frac{\Gamma_h}{k_B T}\right)-1\right]. \qquad (14)$$

Ten parameters are involved, seven ones are already known.
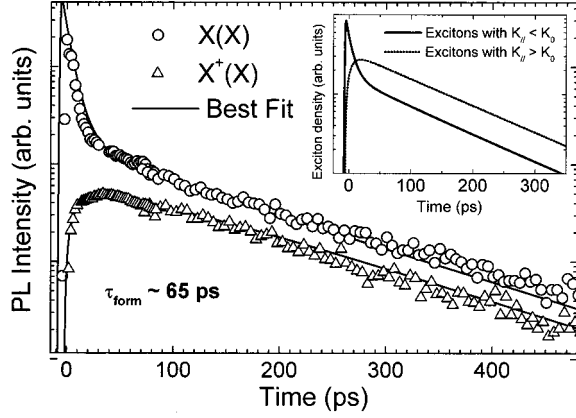
FIG. 9. Fit of the X and X^+ intensity, when exciting the X transition. Inset: calculated populations of the neutral exciton with different wave vectors.

(1) τ_{rad-X^+} is directly given by the $X^+(X^+)$PL dynamics: $\tau_{rad-X^+} = 60$ ps (see Sec. II).

(2) The exciton exchange energy δ is calculated using Refs. 16 and 35 and is found to be ~ 0.14 meV. The details of the calculation are given in the Appendix.

(3) The homogeneous linewidth Γ_H has been measured by four-wave-mixing experiments on the same sample and is found to be 0.07 meV (Ref. 17).

(4) The exciton spin-flip time τ_x is given by the $X(X)$ polarization dynamics without applied magnetic field and was found to be ~ 12 ps (see Sec. II).

(5) The single-particle electron spin-flip time τ_e is given by the $X^+(X^+)$ polarization dynamics without applied magnetic field and was found to be ~ 60 ps (see Sec. II).

(6) τ_h is given by the fit of the $X(X)$ polarization dynamics in an applied magnetic field and was found to be ~ 20 ps (see Sec. III B).

(7) The temperature T of the carriers is supposed to be equal to the bath temperature (1.7 K). Indeed the excitons are generated with $K_\parallel < K_0$ and have to *gain* some energy to spread out to larger K vector. There is no cooling process of the carriers as it would exist in nonresonant experiments.

We are thus left with three adjustable parameters, τ_K, τ_{rad-X}, and τ_{form}, which we determine by fitting the $X(X)$ and $X^+(X)$ PL dynamics (evolution in time and relative intensities). The best fit is shown in Fig. 9. The parameters are $\tau_{rad-X} = 16$ ps (in good agreement with theoretical estimation[36]), $\tau_K = 12$ ps (also in good agreement with values reported previously[13]), and $\tau_{form} = 65$ ps. We have taken into account the fact that the X PL signal is entirely collected thanks to the spectral resolution of the experimental setup (3 meV) while it is not the case for the X^+ PL signal due to the low-energy tail of the X^+ PL. The $X^+(X)$ signal intensity obtained with the model has thus been divided by a factor 1.5.

The inset in Fig. 9 shows with the solid line the $K_\parallel < K_0$ exciton density ($|\pm 1\rangle$ and $|\pm 2\rangle$ states) and with the dashed line the $K_\parallel > K_0$ exciton density. The density of $K_\parallel < K_0$ excitons, which are the only ones involved in the X^+ formation process, rapidly decreases with a time constant of about 13 ps during the first few tens picoseconds. This time is much shorter than the formation time of the X^+ and than the ra-
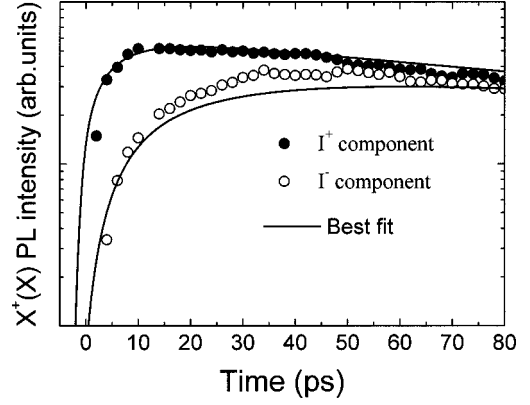
FIG. 10. Experimental (circles) and calculated (lines) rise of the charged exciton PL.

diative lifetime of the X^+. As a consequence, the rise of the $X^+(X)$ PL signal reflects only the rapid decay of the $K_\parallel < K_0$ density of excitons and not the formation time of the X^+. On the other hand, the $K_\parallel > K_0$ excitons become rapidly the main populated states and form a reservoir of nonradiative excitons.

We would like to stress that the present model does not take into account some features which are known to exist. As explained before τ_h should be k dependent and hence time dependent. The excitonic radiative lifetime τ_{rad-X}, also, should increase with time, due to localization.[36] In spite of this oversimplification, which prevents us from obtaining a fully quantitative agreement, the model explains well the main features of the X-X^+ dynamics. In particular, Fig. 10 focuses on the rise of the σ^+ and σ^- components of the $X^+(X)$PL signal. The agreement between the experiment and the calculation is again good, which confirms that the formation of X^+ does not modify the electron spin orientation of the original X.

V. CONCLUSION

The analysis of the charged exciton spin quantum beats in a transverse magnetics field as well as the decay of its photoluminescence polarization have allowed us to conclude that the formation of a charged exciton from an exciton state does not affect either the electron-spin orientation nor its coherence. The exciton spin-flip time as well as the single-particle electron spin-flip time have been measured and we have found 12 and 60 ps, respectively. We have improved the model developed by Dyakonov *et al.*[12] in order to analyze in detail the exciton spin quantum beats observed under a transverse magnetic field and we have extracted the single-particle hole spin-flip time (20 ps). We also have been able to explain why the X polarization can be higher under a transverse magnetic field than without field.

Thanks to the resonant excitation of the X^+ transition, the X^+ radiative lifetime has been directly measured and has been found to be ~ 60 ps. We have used an eight-level model[13] to extract the formation time of the charged exciton after a resonant X excitation. We have found $\tau_{form} \sim 65$ ps. Only three adjustable parameters were used to fit the $X(X)$ and $X^+(X)$ PL dynamics (evolution in time and relative intensities).

ACKNOWLEDGMENTS

APPENDIX: CALCULATION OF THE EXCHANGE ENERGY SPLITTING BETWEEN THE EXCITON STATES

Kusrayev *et al.*[35] measured this splitting in a 20- and a 40-Å width $CdTe/Cd_{0.79}Mg_{0.21}Te$ QW. They found $\delta = 0.5$ and 0.26 meV, respectively. On the other hand, Blackwood *et al.*[16] have calculated the enhancement (F_{ex}) of the exchange interaction in $GaAs/Ga_xAl_{1-x}As$ and $In_{1-x}Ga_xAs/GaAs$ QW's with respect to the bulk material.

In order to estimate the exchange energy in the present 80-Å $CdTe/Cd_{0.69}Mg_{0.23}Zn_{0.08}Te$ QW we have calculated F_{ex} for the 40-Å width $CdTe/Cd_{0.79}Mg_{0.21}Te$ QW and for our sample. We then deduced the bulk value of δ for CdTe (we found 0.095 meV) and its value for the present sample. We found $\delta = 0.14$ meV.

The calculation of the QW electron and hole wave func-

tions are performed using the method developed in Ref. 37, which also allows us to find the dispersion curves of the valence band and thus the effective hole mass in the plane of the QW's. We did not consider the δ value measured for the 20-Å $CdTe/Cd_{0.79}Mg_{0.21}Te$ QW because the extension of the electron and hole wave functions in the barrier is important (40% and 20% of the probability of presence, respectively). As the material parameters (Luttinger coefficient and electron mass) remain largely unknown for $Cd_{1-x}Mg_xTe$ alloys, F_{ex} cannot be determined with a good accuracy. Let us finally point out that the value of δ has only a weak influence on the analysis of the polarization behavior (Secs. IV A and IV B) but has more influence on the analysis of the PL dynamics (Sec. III D). Indeed the thermal equilibrium between the population of $|\pm 1\rangle$ and the $|\pm 2\rangle$ excitons depends critically on this parameter because the temperature is very close to this value. For reasonable values of $\delta (0.1 < \delta < 0.18)$ we are also able to obtain a good fit of the $X(X)$ and $X^+(X)$ PL dynamics by slightly varying τ_K and τ_{rad-X} while τ_{form} is almost unchanged.

[1] K. Kheng, R. T. Cox, Y. Merle d'Aubigné, F. Bassani, K. Saminadayar, and S. Tatarenko, Phys. Rev. Lett. **71**, 1752 (1993).

[2] M. Hayne, C. L. Jones, R. Bogaerts, C. Riva, A. Usher, F. M. Peeters, F. Herlach, V. V. Moshchalkov, and M. Henini, Phys. Rev. B **59**, 2927 (1999).

[3] D. Gekhtman, E. Cohen, Arza Ron, and L. N. Pfeiffer, Phys. Rev. B **56**, R12768 (1997).

[4] G. Finkelstein, H. Shtrikman, and I. Bar-Joseph, Phys. Rev. Lett. **74**, 976 (1995).

[5] G. Eytan, Y. Yayon, M. Rappaport, H. Shtrikman, and I. Bar-Joseph, Phys. Rev. Lett. **81**, 1666 (1998).

[6] R. J. Warburton, C. S. Dürr, K. Karrai, J. P. Kotthaus, G. Medeiros-Ribeiro, and P. M. Petroff, Phys. Rev. Lett. **79**, 5282 (1997).

[7] G. Finkelstein, V. Umansky, I. Bar-Joseph, V. Ciulin, S. Haacke, J-D. Ganière, and B. Deveaud, Phys. Rev. B **58**, 12 637 (1998).

[8] D. Brinkmann, J. Kudrna, P. Gilliot, B. Hönerlage, A. Arnoult, J. Cibert, and S. Tatarenko, Phys. Rev. B **60**, 4474 (1999).

[9] H. P. Wagner, H. P. Tranitz, and R. Shuster, Phys. Rev. B **60**, 15 542 (1999).

[10] P. Kossacki, V. Ciulin, J. Cibert, Y. Merle d'Aubigné, A. Arnoult, C. Bourgognon, A. Wasiela, S. Tatarenko, J-L. Staehli, J. D. Ganière, B. Deveaud, and J. A. Gaj, Proceedings of The Ninth International Conference on II-VI Compounds, Kyoto, 1999 [J. Cryst. Growth (to be published)].

[11] T. Amand, X. Marie, P. Le Jeune, M. Brousseau, D. Robart, and J. Barrau, Phys. Rev. Lett. **78**, 1355 (1997).

[12] M. Dyakonov, X. Marie, T. Amand, P. Le Jeune, D. Robart, M. Brousseau, and J. Barrau, Phys. Rev. B **56**, 10 412 (1997).

[13] A. Vinattieri, J. Shah, T. C. Damen, D. S. Kim, L. N. Pfeiffer, M. Z. Maialle, and L. J. Sham, Phys. Rev. B **50**, 10 868 (1994).

[14] A. Haury, A. Arnoult, V. A. Chitta, J. Cibert, Y. Merle d'Aubigné, S. Tatarenko, and A. Wasiela, Superlattices Microstruct. **23**, 1097 (1998).

[15] A. Arnoult, D. Ferrand, V. Huard, J. Cibert, C. Grattepain, K. Saminadayar, C. Bourgognon, A. Wasiela, and S. Tatarenko, J. Cryst. Growth **202**, 715 (1999).

[16] E. Blackwood, M. J. Snelling, R. T. Harley, S. R. Andrews, and C. T. B. Foxon, Phys. Rev. B **50**, 14 246 (1994).

[17] The present sample has also been studied in the same FWM experiment as in Ref. 10. The results are similar to the ones presented in this paper and allows us to conclude on the localization of the X^+ in the QW's of interest for the present study.

[18] X. Marie, P. Le Jeune, T. Amand, M. Brousseau, J. Barrau, and M. Paillard, Phys. Rev. Lett. **79**, 3222 (1997).

[19] B. Deveaud, F. Clérot, N. Roy, K. Satzke, B. Sermage, and D. Katzer, Phys. Rev. Lett. **67**, 2355 (1991).

[20] B. Stébé, E. Feddi, A. Ainane, and F. Dujardin, Phys. Rev. B **58**, 9926 (1998).

[21] M. Z. Maialle, E. A. de Andrada e Dilva, and L. J. Sham, Phys. Rev. B **47**, 15 776 (1993).

[22] H. W. van Kesteren, E. C. Cosman, and W. A. van de Poel, Phys. Rev. B **41**, 5283 (1990).

[23] V. F. Sapega, M. Cardona, K. Ploog, E. L. Ivchenko, and D. N. Mirlin, Phys. Rev. B **45**, 4320 (1992).

[24] X. Marie, T. Amand, P. Le Jeune, M. Paillard, P. Renucci, L. E. Golub, V. D. Dymnikov, and E. L. Ivchenko, Phys. Rev. B **60**, 5811 (1999).

[25] A. P. Heberle, W. W. Rühle, and K. Ploog, Phys. Rev. Lett. **72**, 3887 (1994).

[26] Q. X. Zhao, M. Oestreich, and N. Magnea, Appl. Phys. Lett. **69**, 3704 (1996).

[27] C. Y. Hu, W. Ossau, D. R. Yakovlev, G. Landwehr, T. Wojtowicz, G. Karczewski, and J. Kossut, Phys. Rev. B **58**, R1766 (1998).

[28] A. A. Sirenko, T. Ruf, M. Cardona, D. R. Yakovlev, W. Ossau, A. Waag, and G. Landwehr, Phys. Rev. B **56**, 2114 (1997).

[29] B. B. Goldberg, D. Heiman, and A. Pinczuk, Phys. Rev. Lett. **63**, 1102 (1989).

[30] R. M. Hannak, M. Oestreich, A. P. Heberle, W. W. Rühle, and K. Köhler, Solid State Commun. **93**, 313 (1995).

[31] C. Cohen-Tannoudji, J. Dupont-Roc, and G. Grynberg, *Processus d'Interaction entre Photons et Atomes*, Savoirs actuels

(InterEditions/Editions du CNRS, Paris, 1988).

[32] M. I. Dyakonov and V. Yu. Kachorovskii, Fiz. Tekh. Poluprovodn. **20**, 178 (1986) [Sov. Phys. Semicond. **20**, 110 (1986)].

[33] P. Kossacki, J. Cibert, D. Ferrand, Y. Merle d'Aubigné, A. Arnoult, A. Wasiela, S. Tatarenko, and J. A. Gaj, Phys. Rev. B **60**, 16 018 (1999).

[34] M. Oestreich, D. Hägele, J. Hübner, and W. Rühle, Phys. Status Solidi A **178**, 27 (2000).

[35] Yu. G. Kusrayev, B. P. Zakharchenya, G. Karczewski, T. Wojtowicz, and J. Kossut, Solid State Commun. **104**, 465 (1997).

[36] D. S. Citrin, Superlattices Microstruct. **13**, 303 (1993).

[37] G. Fishman, Phys. Rev. B **52**, 11 132 (1995).